Vol 15 No 2, February 2006
1009-1963/2006/15(02)/0432-05

Chinese Physics

© 2006 Chin. Phys. Soc.
and IOP Publishing Ltd

X-ray diffraction study of effect of deposition conditions on α–β phase transition and stress evolution in sputter-deposited W coatings

Wang Cong(王 聪)[a)b)], Brault Pascal[a)†], Pineau Alain[c)], Plantin Pascale[a)], and Thomann Anne-Lise[a)]

[a)] *Groupie de Recherches sur l'Energétique des Milieux Ionisés UMR6606 -CNRS, Ecole Polytechnique de l'Université d'Orléans, BP6744 Université d'Orléans, F-45067 Orléans, Cedex 2, France*

[b)] *School of Science, Beijing University of Astronautics and Aeronautics, Beijing 100083, China*

[c)] *Centre de Recherches sur la Matière Divisée – UMR 6619 CNRS – Université d'Orléans, 1B rue de la Férollerie, 45071 Orléans, Cedex 2, France*

(Received 26 May 2005; revised manuscript received 7 November 2005)

Pure W and W–Cu–W trilayer coatings were deposited on an Fe substrate by d.c. magnetron sputtering. The $\alpha-\beta$ phase evolution, intragranular stress evolution in sputter-deposited W layer were investigated by x-ray diffraction. They are directly related to the film microstructure, density and adhesion. Therefore, control of the film stress and phase component transition is essential for its applications. The phase component transition from β-W to α-W and intragranular stress evolution from tensile to compressive strongly depend on the deposition parameters and can be induced by lowering Ar pressure and rising target power. The compressively stressed films with α-W phase have a dense microstructure and high adhesion to Fe substrate.

Keywords: W coatings, x-ray diffraction, α–β phase component transition, thin film stress
PACC: 6855, 8115C, 3320R, 8160

1. Introduction

W coatings have important applications in many fields, like microelectronics,[1–3] high temperature shielding,[4] armour as plasma and nuclear-interaction components.[5–7] W–Cu is an attractive candidate material for the heat-sink as well as armour. However, densification in microstructure and improved mechanical properties remain required for the applications.

There are two crystalline phases of W:[8] thermodynamically stable α-W and metastable β-W phase. α-W phase has a body-centred-cubic (bcc) structure and a higher density (19.3 g.cm^{-3}); whereas β-W phase, of W_3O or W_3W type, has an A15 primitive cubic structure and a lower density (14.6g·cm^{-3}). The β-W phase is usually stabilized by oxygen impurities. This oxygen incorporation results in volume variation of the film, which certainly induces low density, worse adhesion and other bad mechanical properties. So, control of the β phase nucleation is essential for assuring required thin film properties. Ligot *et al* and Villain *et al* [2,8] have investigated the microstructure, $\alpha-\beta$ phase transition and residual stress in tungsten films on polyimide and obtained some valuable results. Wang and Wang *et al* [9] reported a dense W–Cu multilayer coating deposited on Fe substrate by magnetron sputtering.

The intrinsic stress is another important factor for film mechanical properties, which comes from lattice mismatch, impurities, grain boundaries and other defects. The tensile-compressive stress transition of sputter- deposited metal films as a function of sputtering gas pressure was studied by Thornton and Hoffman.[10] The development of compressive stress is attributed to high energy bombardment of the growing film due to an "atomic peening" process. The stress transition is a function of the pressure and target/substrate distance. In the sputter-deposition process, the atomic peening effect can be enhanced/reduced by two means:[11] (1) by increas-

†Corresponding author: Pascal.Brault@univ-orleans.fr

ing/decreasing the number of incident energetic particles (the energetic ion or neutral flux j), or (2) by increasing/decreasing the incident energy, ξ of the incident particles. Under the assumption of atomic peening, Windischmann[12] has suggested the compressive stress σ:

$$\sigma \propto j\xi^{1/2}.$$

Thus the film stress can be controlled by controlling deposition flux and energy, which can be changed by varying target power and sputtering pressure.

In the present investigation, direct current (DC) magnetron sputtering was employed to prepare W or W–Cu–W coatings on Fe substrates. The $\alpha - \beta$ phase transition and state of residual stress in the films were investigated by x-ray diffraction, accompanied by SEM observation, Rutherford backscattering spectroscopy (RBS) measurement and scotch test, as a function of the sputtering gas pressure $P_{\rm r}$ and target power P.

2. Experiment

A magnetron sputtering system (APRIM VIDE) with three independent DC planar magnetron targets was used to sputter W and Cu (one target being idle), which had also been described in Ref.[9]. The target disc diameter is 100 mm and the square substrate has an area of $100\times100\,{\rm mm}^2$. The target to substrate distance is kept fixed at 9 cm for each deposition run. The base ultrahigh vacuum (UHV) in the deposition chamber was maintained below 10^{-5} Pa by a turbo molecular pump (ATP900, ALCATEL). The Fe substrate, after a treatment of ultrasonic pre-cleaning in acetone solution, was UHV transferred into the sputtering vacuum chamber. Prior to the deposition, the targets were pre-sputtered for a few minutes to remove any contamination on the surface.

A Philip's X'Pert Pro XRD (PW1830 generator and PW3020 goniometer) equipment using Cu$K\alpha$ radiation (λ=1.541837 Å) at 40kV / 30mA was used for crystal structure analysis. The scanning step was 0.04° and scanning time for every step was 2.5s. The 2θ scanning range was from 32° to 60° or extend to 68° in a continuous scanning mode. Surface morphology and film thickness were measured by scanning electron microscopy (SEM) (using Hitachi: S-4200 instrument). The film density were assessed by RBS using 2.0 MeV $^4{\rm He}^+$ ions in a van de Graaff accelerator. Film adhesion was evaluated by scotch test.

3. Results and discussion

There are 10 kinds of samples with either W single layer or W–Cu–W trilayer structure, denoted by No.1–9, prepared by d.c. magnetron sputtering with different deposition parameters, which were shown in Table 1. The sample No.5* has the same W-layer as the sample No.5 and an addition of the Cu layer sandwiched between two W-layers. The cross sectional SEM images of W single layer and W–Cu–W trilayer films are shown in Fig.1(a, b). At first, pure W coatings were deposited on Fe substrates by changing Ar pressure from 0.2 Pa to 2.5 Pa and fixing target power at 500 W. The XRD patterns of 4 kinds of samples (corresponding to No.1, 3, 5, 7) are shown in Fig.2. From JCPDF card (No. 04-806) using Cu$K\alpha$ radiation, α-W has only two x-ray diffraction peaks in the range from 2θ=32° to 60°: 2θ =40.262 (110), 58.272 (200); whereas β-W has three peaks: 2θ=35.525 (200), 39.885 (210), 43.880 (211) from JCPDF card (No.47–1319). Fe, as substrate material, belongs to bcc lattice type and has two XRD peaks: 2θ=44.675 (110) and 65.026 (200) in the 2θ scanning range. The strongest peaks of α-W and β-W always overlap, and fortunately α-W has a peak at 2θ=58.3° and β-W has a peak at 2θ=35.5° by which we can distinguish the phases. As seen in Fig.2, the samples No.1 and No.3 have mixed α-W and β-W phases and No.5 and No.7 show pure α-W phase. With lowering Ar pressure, $\beta - \alpha$ phase component transition occurs in the Ar pressure range from 1.5 Pa to 1.0 Pa, independent of the thickness, while the sputtering power on the tungsten target is 500 W. Villain *et al* [8] reported that pure α-W phase was found in the 600 nm films on polyimide substrates and co-existence of α-W and β-W phases happened in 200 nm films. However. in our experiments, the α-W phase formation on Fe substrates is much dependent on the deposition parameters, but not film thickness. Fig.3 shows the XRD patterns of the samples in W/Cu/W trilayer structure on Fe substrates with changing target power and film thickness and keeping the constant sputtering pressure (1.0 Pa), which correspond to samples No.4 and No.5*. It can be seen that for the sample No.4 a higher peak (200) of β-W phase occurs with lower target power (200 W), despite the W-layer thickness is 600 nm. We know that β phase formation is favoured by a weak energy of incident particles and a low deposition rate, accompanied by oxygen incorporation, which correspond to high Ar pressure and low target power. On the contrary, with higher target power (500 W), a pure α-W

phase exists in a 285 nm W-layer which was displayed in the sample No.5* and No.5.

Table 1. Deposition parameters of 10 kinds of samples and the shift ($\Delta\ 2\theta$) of the XRD peak positions from their standard values of W or W-Cu coatings with changing target power and Ar pressure.

sample number	dep. para. (power, pressure)	W-layer thickness/nm	$\Delta(2\theta) = (2\theta - 2\theta_0)/(°)$			
			β-W(200) (35.525)	α-W(110) (40.262)	Cu(111) (43.317)	Fe(110) (44.675)
01	500, 2.5	970	–0.052	–0.024	–	0
02	500, 2.0	470	+0.028	+0.070	+0.001	0
03	500, 1.5	1000	+0.004	+0.009	–	0
04	200, 1.0	600	+0.040	+0.086	+0.019	0
05	500, 1.0	285		+0.027	–	0
05*	500, 1.0	285		+0.027	+0.090	0
06	500, 0.5	297		–0.040	+0.007	0
07	500, 0.2	400		–0.235	–	0
08	700, 0.2	285		–0.226	+0.047	0
09	750, 0.15	1152		–0.204	–	0

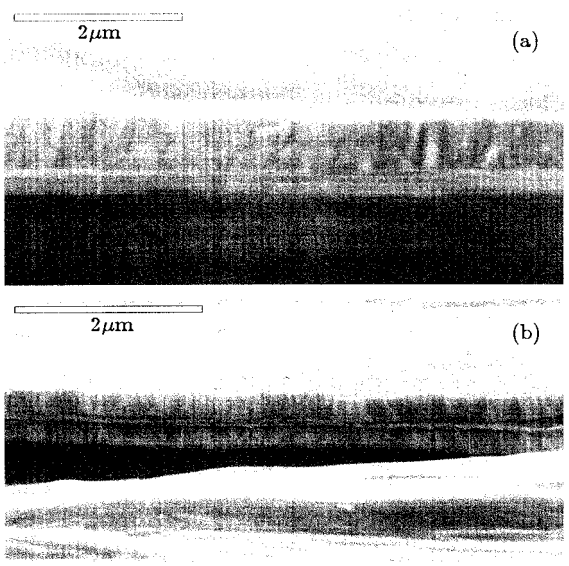


Fig.1. SEM cross sectional images of W and W–Cu coatings ((a): pure W single layer; (b): W–Cu–W trilayer).

On the other hand, it was found from the XRD patterns, taken under the same condition, as shown in Fig.2 and Fig.3, that the relative peak (110) intensity for α-W phase increased greatly when pure α phase was formed, which means good crystallization and increasing content of α-W phase. With the formation of β phase, the relative peak intensities decreased obviously. From the peak shape, we cannot find apparent correlation between the full width at half maximum (FWHM) of the peaks and the deposition parameters, but the α-W peak indicates greater broadening of FWHM and the highest relative intensity only when the Ar pressure is lower than 0.2 Pa, which is seen in Fig.2 (sample No.7). The mean crystalline size is estimated to be 20 nm using the FWHM of (110) (2θ=40.262) peak by Scherrer's equation: d=0.89λ/Bcosθ.

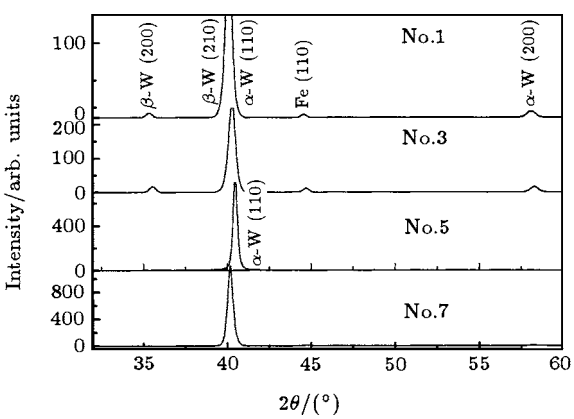


Fig.2. XRD patterns of pure W coatings on Fe substrates with changing Ar pressure and fixed target power (500 W) (No.1: 2.5 Pa; No.3: 1.5 Pa; No.5: 1.0 Pa; No.7: 0.2 Pa).

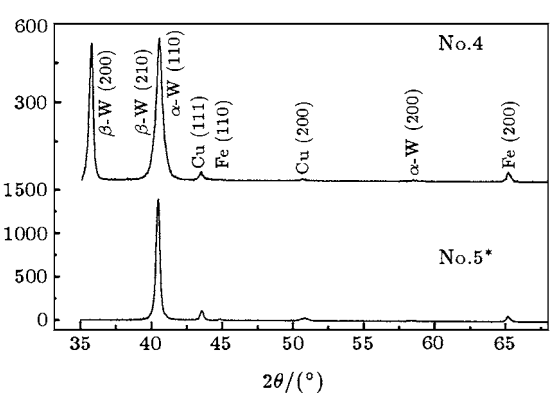


Fig.3. XRD patterns of W–Cu–W multilayer coatings on Fe substrates with changing target power, film thickness and fixed Ar pressure (1.0 Pa) (No.4: 200 W, 600 nm; No.5*: 500 W, 285nm).

The surface morphology was observed by SEM. Fig.4 shows the different W-surface morphology under the different Ar pressure and the finer grains and denser microstructure were formed at lower pressure. The crystal size of about 25 nm by SEM observation is in agreement with the XRD results. Rutherford backscattering spectroscopy (RBS) and scotch tests verified that the W-coatings prepared using lower pressure and higher target power have a high density close to its bulk density and excellent adhesion, which has been reported in a previous paper.[9]

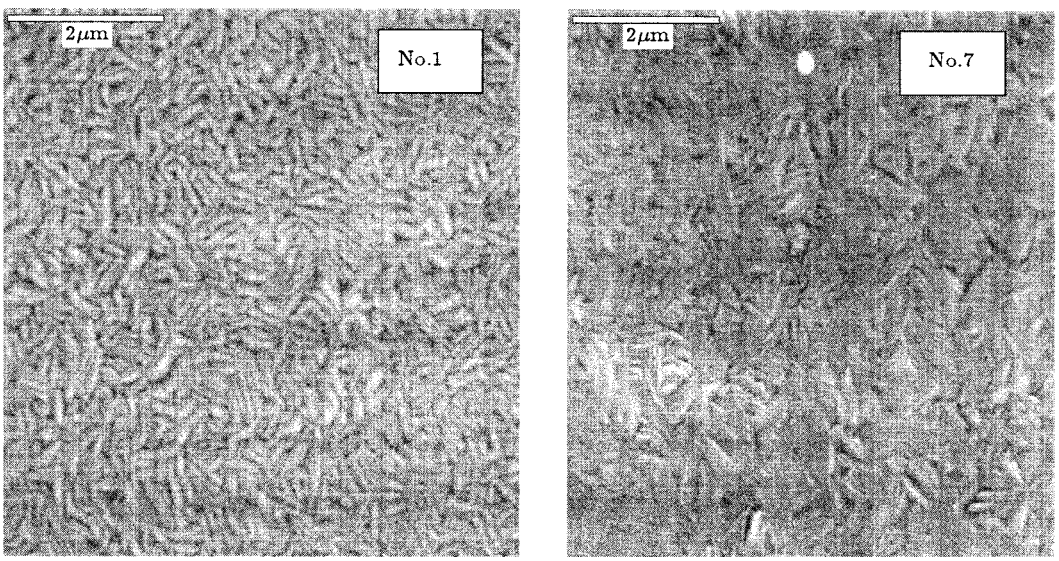


Fig.4. Comparison of W surface microstructure observed by SEM showing finer grains and dense structure formed with lower Ar pressure (No.1: 500 W, 2.5 Pa; No.7: 500 W, 0.2 Pa).

XRD patterns show also the difference in the d-spacing of diffraction planes with variable deposition parameters. This can be explained qualitatively by the change of the intragranular stress in the films. An estimate of the sum of principal stresses in the film was made via the simplified well-known formula:[13]

$$\Delta\sigma = -\frac{E_{\mathrm{f}}}{\upsilon_{\mathrm{f}}}\left(\frac{d_{hkl}-d_0}{d_0}\right),$$

where υ_{f} and E_{f} are Poisson's ratio and Young's modulus, respectively, of the film. d_{hkl} and d_0 are the interplanar (hkl) spacing of the stressed and unstressed films. Because of the complexity of the stress determination, mainly due to the polycrystalline nature of the samples, this simple approach merely gives an idea of the magnitude of the stresses in the films. A simple biaxial residual stress in the plane of the film is hereby assumed. This assumption is valid since the samples are partially or fully stabilized in a cubic lattice. Therefore, it is assumed that any shear stress or stress profiles are negligible. When the diffraction peak (110) of the substrate Fe was assumed to be fixed, by which the zero-shift can be calibrated, the shift of 2θ from α-W, β-W and Cu standard peaks can be observed, as shown in Table 1. Ten kinds of samples from No. 1 to 9 were analysed with different W layer thickness, variable target power and Ar pressure. Apparently the XRD peak position shift $\Delta(2\theta)$ of α-W has an evolution from moving to larger 2θ angle $(+\Delta)$ to moving to smaller angle $(-\Delta)$, relative to their standard value from JCPDF card, when lowering Ar pressure or increasing target power. Only there is exception for the sample No.1, for which the reason is not clear. This implies an evolution from tensile stress $(+\sigma)$ to compressive stress $(-\sigma)$, whereas the 2θ shift of Cu peaks always remains positive, which means that there always exists tensile stress in the Cu layer despite the changing target power and pressure, the β-W phase is mostly under tensile stress, except for the deposition conditions of overhigh pressure. The tensile-stressed films indicate the presence of voids in the films. This kind of defect tends to shrink the film due to the high surface tension of the inner surface of the voids, as a result, the tensile stress is generated.[14] The voids must be related to oxygen, and thus β-W. This is in agreement with the phase analysis by XRD. So the tensile stress is due to β-W phase formed un-

der higher Ar pressure and lower target power. Using Bragg's equation, $2d\sin\theta = n\lambda$, we obtain:

$$\Delta d = -d \text{ ctg } \theta \Delta\theta.$$

For α-W, lattice constant a=3.165Å, d=2.238Å and θ=20.13° for its maximum XRD peak (110), thus Δd=–6.109 $\Delta\theta$. As a result, it was found that the XRD peaks generally shift to larger d-spacing with decreasing sputtering pressure, which is in agreement with most reports, such as Refs.[8, 9, 15]. Film adhesion is closely related to intrinsic stress. By scotch test, the lower the pressure, the stronger the film adhesion on the Fe substrate. Lowering Ar pressure means to increase the high energy deposition, and high-energy deposition creates compressive residual stress by atomic peening.[16] In contrast, with tensile stress, the adhesion is not so good. On the other hand, film density measurement by RBS shows that, with high target power and low Ar pressure, the W film has higher density. This has been discussed in detail in a separated paper.[17] High target power would increase the sputtering rate and thus deposition rate. Shen[14] reported that a MoN_x film contains a dense microstructure which is responsible for the observed compressive stress at lower sputtering pressure, which is in agreement with our results.

4. Conclusion

For W coatings, the control of phase component transition from β-W to α-W and film stress are important for the coating density and coating adhesion. By x-ray diffraction, we observed the phase component transition and stress evolution resulting from changing deposition parameters in a d.c. magnetron sputtering deposition process. Gaining higher density α-W phase and compressive stress with lower Ar working pressure and higher target power is responsible for the high density coating and good adhesion. These transitions were discussed from the view point of film microstructure and deposition process.

Acknowledgement

C. Wang would like to thank Région Centre for a research fellowship. CME - Université d'Orléans is acknowledged for the SEM measurements. CRT Plasma – Laser is acknowledged for partial funding. Thanks to A. Richard (CME, University of Orleans) for help in SEM measurements.

References

[1] Paturaud C, Farges G, Sainte Catherine M C and Machet J 1996 *Surf. Coat Technol.* **86–87** 388
[2] Ligot J, Benayoun S, Hantzpergue J J and Remy J C 1999 *Solid-State Electronics* **43** 1075
[3] Kim Young Do, Oh Nang Lyeom, Oh Sung-Tag and Moon In-Hyung 2002 *Mater. Lett.* **51** 420
[4] Itoh Yoshiyasu, Takahashi Masashi and Takano Hirohisa 1996 *Fusion Eng. Design* **31** 279
[5] Davis J W, Slattery K T, Driemeyer D E and Ulrickson M A 1996 *J. Nucl. Mater.* **233–237** 604
[6] Cambe A, Gauthier E, Layet J M and Bentivegna S 2001 *Fusion Eng. Design* **56–57** 331
[7] Montanari R, Riccardi B, Volterri R and Bertamini L 2002 *Mater. Lett.* **52** 100
[8] Villain P, Goudeau P, Ligot J, Benayoun S, Badawi K F and Hantzpergue J J 2003 *J. Vac. Sci. Technol.* A **21** 967
[9] Wang C, Brault P, Zaepffel C, Thiault J, Pineau A and Sauvage T 2003 *J. Phys. D: Appl. Phys.* **36** 2709
[10] Thornton J A and Hoffman D W 1989 *Thin Solid Films* **171** 5
[11] Chiu K F, Barber Z H and Somekh R E 1999 *Thin Solid Films* **343–344** 39
[12] Windischmann H 1987 *J. Appl. Phys.* **62** 1800
[13] Boulouz M, Martin L, Boulouz A and Boyer A 1999 *Mater. Sci. Eng.* B **67** 122
[14] Shen Y G 2003 *Mater. Sci. Eng.* A **359** 158
[15] Kevin Minor M, Crawford T M, Klemmer Timothy J, Peng Yingguo and Laughlin David E 2002 *J. Appl. Phys.* **91** 8453
[16] Kusaka K, Taniguchi D, Hanabusa T and Tominaga K 2002 *Vacuum* **66** 441
[17] Wang C, Brault P and Sauvage T 2005 *Eur. Phys. J.: Appl. Phys.* **31** 17